Journal of the European Ceramic Society **11** (1993) 375–386

Oxidation of Yttria- and Alumina-containing Dense Silicon Nitride Ceramics

Yu. G. Gogotsi, G. Grathwohl, F. Thümmler
Institut für Keramik im Maschinenbau, Universität Karlsruhe, W-7500 Karlsruhe 1, Germany

V. P. Yaroshenko
The Institute for Problems of Materials Science, 252680 Kiev, Ukraine

M. Herrmann & Ch. Taut
Fraunhofer-Einrichtung für Keramische Technologien und Sinterwerkstoffe, O-8020 Dresden, Germany

(Received 2 October 1991; revised version received 21 May 1992; accepted 13 July 1992)

Abstract

The oxidation behaviour of $Y_2O_3 + Al_2O_3$-doped Si_3N_4-based ceramics was investigated in air up to 1500°C under isothermal and non-isothermal conditions. The oxidation resistance of materials is strongly dependent on the content of additives, secondary phases and processing methods, as evident from the behaviour of five materials of the same starting composition prepared by hot-pressing and gas-pressure sintering. Gas-pressure sintered ceramics containing crystalline yttrium–silicon oxynitrides in the intergranular phase showed instability at intermediate temperatures and lower oxidation resistance than hot-pressed ceramics prepared from the same powder mixtures. Hot-pressed ceramics exhibited excellent resistance to oxidation by air at temperatures up to 1400–1450°C, because of the formation of a protective oxide layer. A decrease of oxidation rates with the increase of additives content was found at temperatures below 1300°C, while the reverse was the case for all materials above 1400°C.

Das Oxidationsverhalten der $Y_2O_3 + Al_2O_3$-dotierten Siliziumnitridkeramiken wurde bis 1500°C unter isothermen und nichtisothermen Bedingungen an Luft untersucht. Wie die Untersuchung der jeweils heißgepreßten und gasdruckgesinterten Werkstoffe mit fünf verschiedenen Zusammensetzungen aufgewiesen hat, ist die Oxidationsbeständigkeit der Werkstoffe sehr von dem Gehalt der Sinteradditive, Korngrenzenphasen und Verfahrenstechnik abhängig. Gasdruckgesinterte Keramiken enthalten kristalline Y–Si-Oxynitride in der Korngrenzenphase und zeigen eine niedrige Stabilität bei dazwischenliegenden Temperaturen und eine niedrigere Oxidationsbeständigkeit als heißgepreßte Keramiken der gleichen Zusammensetzung. Dank der Ausbildung der schützenden Oxidschicht weisen heißgepreßte Keramiken sehr gute Oxidationsbeständigkeit an Luft bis 1400–1450°C auf. Die Oxidationsraten bei Temperaturen bis 1300°C nehmen mit zunehmendem Additivgehalt ab. Bei Temperaturen >1400°C findet eine umgekehrte Abhängigkeit statt.

Le comportement à l'oxydation de céramiques à base de Si_3N_4, dopées à l'Y_2O_3–Al_2O_3, a été examiné, dans l'air, jusqu'à 1500°C, en conditions isothermes et non isothermes. La résistance à l'oxydation des matériaux dépend fortement de leur contenu en additifs, des phases secondaires et des méthodes d'élaboration. Ceci est mis en évidence par le comportement de cinq matériaux, de même composition initiale, préparés par compression uniaxiale à chaud et frittage sous pression gazeuse. Les céramiques frittées par pression gazeuse contenant des oxynitrures Y–Si cristallins en tant que phase intergranulaire, ont montré leur instabilité aux températures intermédiaires et une résistance à l'oxydation plus faible que les céramiques de même composition fabriquées par pressage uniaxial à chaud. Ces dernières présentent une excellente résistance à l'oxydation dans l'air jusqu'à des températures de 1400 à 1450°C, en raison de la formation d'une couche d'oxyde protectrice. Une diminution des vitesses d'oxydation est observée avec l'augmentation du contenu en additifs pour les températures inférieures à 1300°C, par contre l'effet inverse est constaté pour tous les matériaux au-dessus de 1400°C.

Journal of the European Ceramic Society 0955-2219/93/$6.00

1 Introduction

Today, high-strength ceramic materials are widely used for engine components, turbochargers, cutting tools, etc. It is well known that silicon nitride is one of the best materials for high-temperature applications. Y_2O_3 and Al_2O_3 sintering aids are most widely used for the preparation of Si_3N_4 ceramics possessing high strength at temperatures higher than 1000°C. In the case of high-temperature engineering applications of Si_3N_4, one of the most important factors affecting the performance is its oxidation behaviour. Therefore the oxidation of Si_3N_4–Y_2O_3–Al_2O_3 ceramics has been studied previously (Table 1).

Thermochemical analysis provided by Luthra[13] indicated that the reaction rates of high-purity Si_3N_4 should be influenced by both diffusion through SiO_2 and an interface reaction. The most favoured interpretation of oxidation phenomena in polyphase Si_3N_4 materials considers that the oxidation rate-controlling process is the sequential inward diffusion of oxygen (to generate silicon oxynitride and silica), and the outward diffusion of intergranular metal oxide as a result of ionic chemical potential gradients.[14] In the temperature range of interest molecular diffusion of O_2 seems to be the major mechanism of oxygen transport through silica or silicate layers.[15] In general, the oxidation resistance of these ceramics depends on the amount of sintering aids used and the composition of a grain-boundary phase. In most of the previous studies the decisive role of diffusion of additive and impurity cations within the grain-boundary phases or diffusion of oxygen and nitrogen through the oxide layer has been stressed. Diffusion processes are indicated as the rate-controlling step for the parabolic oxidation behaviour observed in a range of testing conditions.[1,8–10] However, satisfactory explanations about the logarithmic oxidation kinetics[4,16] and the acceleration of the nitrogen evolution after some period of heating[6,7] have not yet been achieved.

The purpose of this study is to compare and discuss the oxidation behaviour of five materials in the system Si_3N_4–Y_2O_3–Al_2O_3, differing in the content of Y_2O_3 and Al_2O_3 and the type of secondary phases as a consequence of the adapted sintering conditions.

2 Experimental

2.1 Materials

The mechanisms and kinetics of oxidation were investigated using model compositions containing various amounts of yttria and alumina (Fig. 1). High-purity Soviet Y_2O_3 ($d_{50} = 8\ \mu m$) and α-Al_2O_3 ($d_{50} = 2{\cdot}5\ \mu m$) powders were used. Kema Nord silicon nitride powder (α-phase content >90%) and the additives were ball-milled in acetone, using hard alloy (Fe,Co-bonded WC) media, to $d_{50} < 1\ \mu m$ and

Table 1. Survey of oxidation studies

Year	*Reference*	*Processing*	*Additives (mass%)*		*Environment*	*Temperature (°C)*	*Observations*
			Y_2O_3	Al_2O_3			
1980	Hasegawa *et al.*[1]	HP	5	2	Dry O_2	1200–1300	The oxidation is controlled by a diffusion mechanism. Cristobalite, $Y_2Si_2O_7$ and glassy phase are formed.
1980	Quackenbush & Smith[2]	S, HP	3–25	0–2	Air	900–1350	Parabolic oxidation above T_c and a linear one below T_c.
1987	Govila[3]	S	8	2	Air	500–1200	Oxidation at the intermediate temperatures. Pits in the surface layer are observed. $Y_2Si_2O_7$ is formed.
1988	Nickel *et al.*[4]	S	9·8	1·7 (3·5 AlN)	O_2	1200–1465	Logarithmic oxidation. Bubbles formation.
1989	Wang *et al.*[5]	S	13·9	4·5	Air	900–1200	High oxidation resistance, strength improvement after oxidation.
		S	15·0	5·0			
1989	Wakamatsu *et al.*[6,7]	GPS	3·64	2·67	O_2	1400–1600	Mass-spectrometric investigation of exhaust gas was carried out. Acceleration of the oxidation is observed.
		GPS	4·71	4·57			
		GPS	6·71	6·67			
		HIP	5·37	3·64			
1989, 1990	Echeberria & Castro[8,9]	HIP	6	4	Air	1100–1500	Parabolic oxidation, $E = 865$ kJ/mol. Si_2N_2O, β-$Y_2Si_2O_7$ and Y-rich silicate glass are found.
1990	Bellosi *et al.*[10]	HP	8	3	Air	800–1450	Parabolic oxidation, $E = 630$ kJ/mol. Material with Y silicates as intergranular phase starts to oxidize at ~1200°C, with Y oxynitride at 800°C.
		GPS	7	3			
1990	Kim & Moorhead[11]	HIP	6	1·5	Ar–O_2	1400	Cristobalite and/or $Y_2Si_2O_7$ are formed.
1990	Gogotsi *et al.*[12]	HP	5	2	Air	400–1400	Low-temperature oxidation and strength degradation of ceramics with Y oxynitrides.

HP, Hot pressing; S, sintering; GPS, gas-pressure sintering; HIP, hot isostatic pressing.

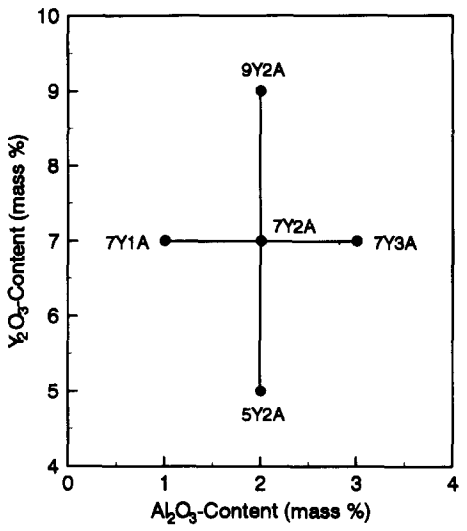

Fig. 1. Compositions under study.

$d_{max} = 4\,\mu m$. WC pick-up from the ball milling was ~2 mass%. The first group of samples (HPSN) was hot pressed at a temperature of 1840°C (0·5 h) in graphite dies without a controlled atmosphere at a pressure of 30 MPa (processed at the Institute for Problems of Materials Science, Kiev, Ukraine).[12] The second group of samples (SSN) was gas-pressure sintered at 1850°C (1·5 h) in nitrogen (processed at the Fraunhofer-Einrichtung für Keramische Technologien und Sinterwerkstoffe, Dresden, Germany).[17] The samples were embedded in Si_3N_4 powder ($d < 100\,\mu m$). The N_2 pressure was held at 0·5 MPa during the ramp and at 5 MPa during the soaking time. Mass loss during sintering was <2%. From the obtained billets the test samples (2 × 5 × 15 mm) were cut and ground with a 100-μm diamond wheel.

The properties of materials used are given in Table 2. All materials possess near theoretical density. $\alpha \rightarrow \beta$ conversion was not complete in HPSN; ~5% of α-Si_3N_4 still remains in the samples owing to the shorter sintering time and lower sintering temperature. As crystalline secondary phases, in HPSN traces of yttrium silicates and in SSN, some $Y_4Si_2O_7N_2$ (YAM in which Si and Y are partly substituted by Al and O), $YSiO_2N$ (wollastonite) and Y-apatite have been identified. WC, WSi_2 and traces of W_5Si_3 and Fe_6W_6C were also found in samples as uniformly distributed inclusions of ~1 μm size. These compounds are present as a result of mixing in the ball mill in WC media. Hot-pressed samples had higher contents of WSi_2. Sintered samples contained preferentially WC, W_5Si_3 and Fe_6W_6C. W, Fe and Co were revealed as major impurities by energy dispersive X-ray microanalysis (EDAX) and wavelength dispersive microanalysis (WDS). The content of other impurities was lower than the sensitivity of the methods used. The oxygen content in sintered specimens was always lower than in hot-pressed ones (Table 2). Chemical analysis of sintered specimens showed that the loss of Y and Al during sintering was rather low (Table 3).

The investigation of polished and etched surfaces demonstrated that the average thickness of the silicon nitride grains a was <0·7 μm (Table 2) and the aspect ratio $c/a \leq 9$.

2.2 Experimental procedure

Oxidation of the ceramics in air under programmed heating up to 1500°C and isothermal conditions was studied using a Netzsch thermobalance capable of 2×10^{-5} g resolution. Non-isothermal conditions (heating rate 2°C/min) were chosen to determine the number of reaction stages and changes in oxidation behaviour with temperature. Other samples were heated to the selected isothermal hold temperature

Table 2. Materials characterization

Material	*Processing*	*Density* (g/cm^3)	*Microstructural characteristics*				*Strength*[a] (*MPa*)	*Oxygen content* (%)	*Excess content of oxygen* (%)[b]
			a_{50} (μm)	c/a (*max*)	*Grains with* $c/a > 4$ (%)	*Grains with* $c/a > 6$ (%)			
5Y2A	HP	3·40	0·43	9	40	27	897[c]	4·21	2·2
5Y2A	S	3·32	0·43	9	40	17	870[d]	3·76	1·8
7Y1A	HP	3·39	0·38	9	42	22	722[c]	n.d.	n.d.
7Y1A	S	3·35	0·66	8	44	23	425[d]	n.d.	n.d.
7Y2A	HP	3·44	0·35	9	39	17	800[c]	4·21	1·8
7Y2A	S	3·36	0·63	9	33	18	822[d]	4·05	1·6
7Y3A	HP	3·41	0·39	9	52	28	746[c]	5·10	2·2
7Y3A	S	3·36	0·66	9	39	19	717[d]	4·00	2·1
9Y2A	HP	3·45	0·40	8	34	15	824[c]	5·15	2·3
9Y2A	S	3·45	0·60	9	30	21	732[d]	5·00	2·1

a, Thickness; *c*, length of β-Si_3N_4 grains; n.d., not determined.
[a] Mean of 10–12 measurements.
[b] Total content of oxygen minus the oxygen content from sintering additives.
[c] Three-point bending.
[d] Four-point bending.

Table 3. Composition of sintered materials

Material	Designated composition				Chemical analysis	
	Y_2O_3 (mass%)	Y (mass%)	Al_2O_3 (mass%)	Al (mass%)	Y (mass%)[a]	Al (mass%)[b]
5Y2A	5	3·94	2	1·06	3·55	1·0
7Y1A	7	5·50	1	0·53	4·66	0·6
7Y2A	7	5·50	2	1·06	5·66	1·2
7Y3A	7	5·50	3	1·59	n.d.	n.d.
9Y2A	9	7·06	2	1·06	6·67	1·0

n.d., Not determined.
[a] Accuracy 0·2%.
[b] Accuracy 0·3%.

at a rate of 20°C/min. The cooling rate was in both cases ~10°C/min. A nearly constant oxidation time of 100 h was maintained for most of the isothermal experiments. All samples were ultrasonically cleaned in acetone and weighed with a microbalance before and after oxidation.

Oxidation products were examined by X-ray diffractometry (XRD) (Siemens, D500), scanning electron microscopy (Cambridge Stereoscan S4-10 and Superprobe 733) and metallography (Zeiss, Axiomat). EDAX and WDS were used to identify the composition of materials and element distribution in oxide layers. XRD peak intensity measurements of the phases were taken for the strongest diffraction signals: (101) for α-cristobalite (SiO_2), (200) for β-Si_3N_4 and (021) for β-$Y_2Si_2O_7$. Relations of the intensities of α-cristobalite or yttrium silicate peaks to the intensity of the strongest β-Si_3N_4 peak were used to normalize the XRD data. Supposing a uniform distribution of oxide phases in the surface layer and formation of thin (<100 μm) oxide films, no other special corrections to the measured XRD peak heights were made. Therefore the XRD results were used only for semiquantitative comparison of the contents of main oxide phases on the surface of different materials and cannot serve as a quantitative measure of the mass or molar content of these phases.

3 Results

In experiments with constant heating rates, the detectable mass gain of hot-pressed samples starts at >1050°C (Fig. 2), and up to ~1400–1450°C oxidation is not very pronounced. When a sample is heated above this point, the mass gain increases rapidly.

Under isothermal conditions no mass gain was detected at temperatures lower than 1050°C, though changes in the surfaces of SSN samples were observed even at lower temperatures. No oxidation of silicon nitride can be detected at these temperatures according to XRD; only the decomposition and reaction of Y–Si oxynitrides are involved in the process.

The mass gain versus time curves for some of the tested materials oxidized at 1300–1500°C (Figs 3 and 4) approximate to the classical parabolic behaviour represented by the equation

$$(\Delta m/S)^2 = k_p t \qquad (1)$$

but only in limited time intervals.

The evaluation of the content of crystalline phases in the samples oxidized at 1200 and 1350°C as derived from semiquantitative XRD is reported in Fig. 5. XRD analysis of the surfaces of samples showed the presence of α-cristobalite and yttrium disilicate (β-$Y_2Si_2O_7$). Mullite was found only after oxidation at 1500°C.

Oxide surface layer morphology developed on samples at >1100°C (examples in Fig. 6 for SSN and in Fig. 7 for HPSN) shows features which are similar to those observed for other Si_3N_4-based materials.[10,18] The reaction product formed at $T \geq 1200$°C is essentially the same for all samples and shows the development of preferentially oriented plate-like crystals of β-$Y_2Si_2O_7$ (Fig. 7, bright) with different morphologies in a glassy viscous phase (dark). The diffusion of the additive cations (Al and Y) and of the impurity cations (Na, K and Ca) is very pronounced. This leads to the

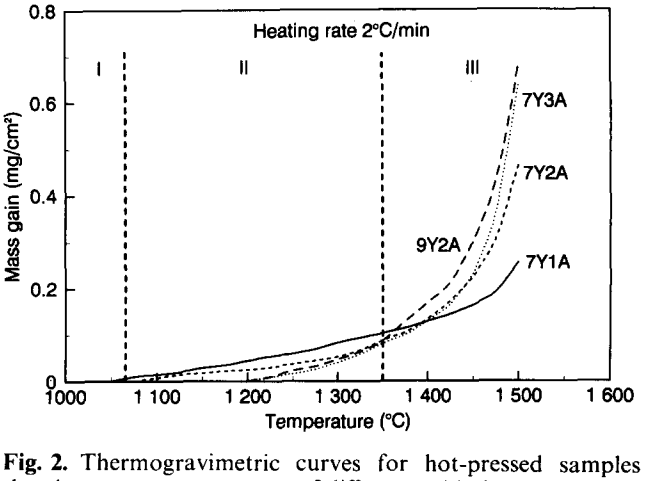

Fig. 2. Thermogravimetric curves for hot-pressed samples showing temperature ranges of different oxidation behaviours.

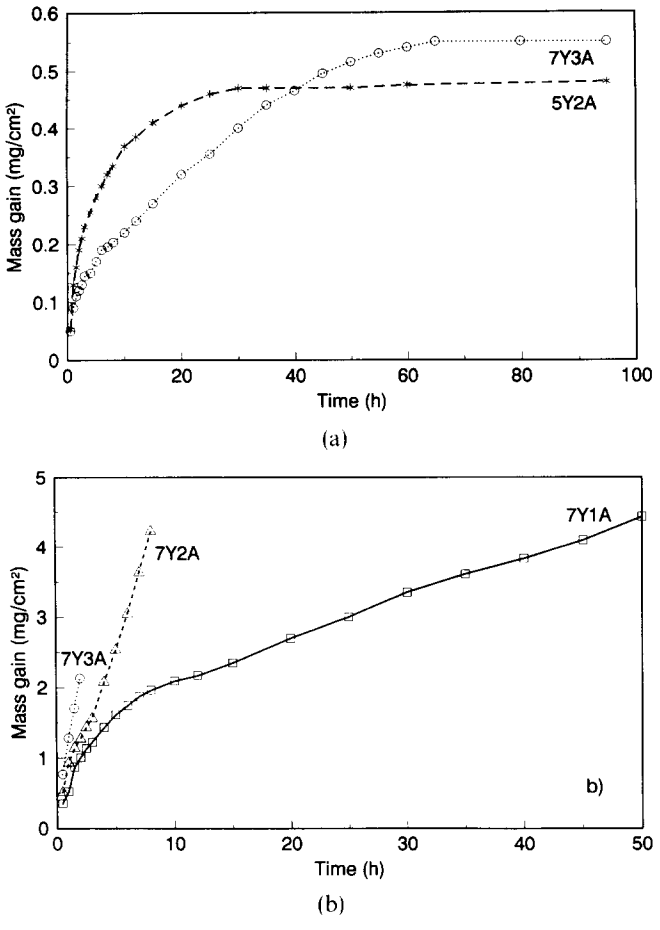

Fig. 3. Oxidation kinetic curves for hot-pressed ceramics of different compositions at (a) 1300°C and (b) 1500°C.

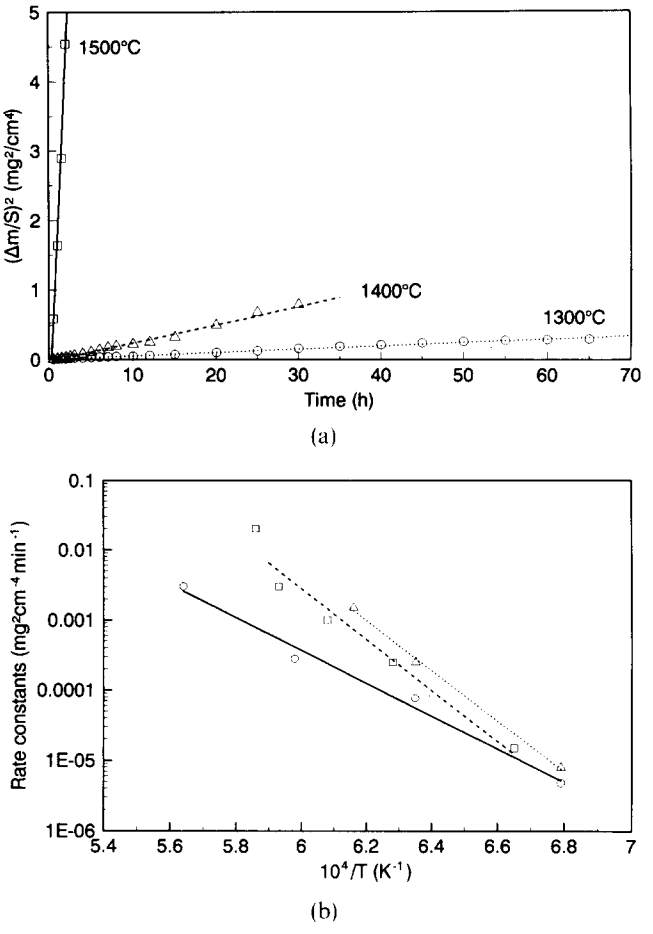

Fig. 4. (a) Oxidation kinetic curves for hot-pressed 7Y3A samples at different temperatures. (b) Arrhenius plot of the parabolic rate constants: —○—, HPSN 7Y3A; – –□– –, HPSN 8Y3A;[10] ···△···, SSN 7Y3A.[10]

formation of a glassy silicate layer on the sample surface.[10] However, below ~1400°C, the formation of uniformly thick 'fish-scale'[19] type cristobalite film on HPSN samples was observed (Fig. 8(b)).

The cross-section of a sample 7Y1A oxidized at 1500°C (Fig. 9(a)) shows an example of the glassy scale, containing yttrium silicate crystals (white) and bubbles. A distribution of elements at the boundary oxide layer/substrate is shown in Fig. 10. Above ~1400°C (this temperature is probably near to the eutectic temperature for the silicate layer formed) the viscosity of the oxide scale decreases strongly, and large pores and bubbles form on the surface (Fig. 9). After a short period of initial parabolic oxidation (Fig. 4) the materials oxidized almost linearly (Fig. 3(b)).

Three different oxidation regimes, conditioned by the features of oxidation of ceramics at different temperatures (Fig. 2), can be identified: I—low ($T<$ 1050°C); II—intermediate (1100°C $< T <$ 1300°C); and III—high ($T>$ 1350°C) temperature.

4 Discussion

4.1 Effect of alumina and yttria content

EDAX investigations of an amorphous grain-boundary phase in triple points in both types of materials have shown the presence of all ceramic elements (Si, N, O, Y and Al). However, the measured oxygen content in SSN was lower than in HPSN (Table 2). Thus, the SiO_2 content in the grain-boundary phase in SSN is also lower than in HPSN. This seems to be the main reason for the presence of different crystalline intergranular phases in the two kinds of materials under study. It is known[20] that the oxynitride crystalline phases oxidize at intermediate temperatures more easily than the SiO_2-rich oxynitride glass. At relatively low temperatures (<1100°C) the phases $Y_4Si_2O_7N_2$, $YSiO_2N$ and Y-apatite ($Y_5(SiO_4)_3N$), revealed in SSN by XRD, are also oxidized. For the oxynitride phases observed in SSN, the equations for oxidation are:

$$4Y_5(SiO_4)_3N + 3O_2 = 2Y_2Si_2O_7 + 8Y_2SiO_5 + 2N_2 \quad (2)$$

(volume change 11%[20]),

$$4YSiO_2N + 3O_2 = 2Y_2Si_2O_7 + 2N_2 \quad (3)$$

(volume change 10%[20]) and

$$2Y_4Si_2O_7N_2 + 3O_2 = 4Y_2SiO_5 + 2N_2 \quad (4)$$

Further interaction with the excess of SiO_2 at higher temperatures usually leads to the formation of

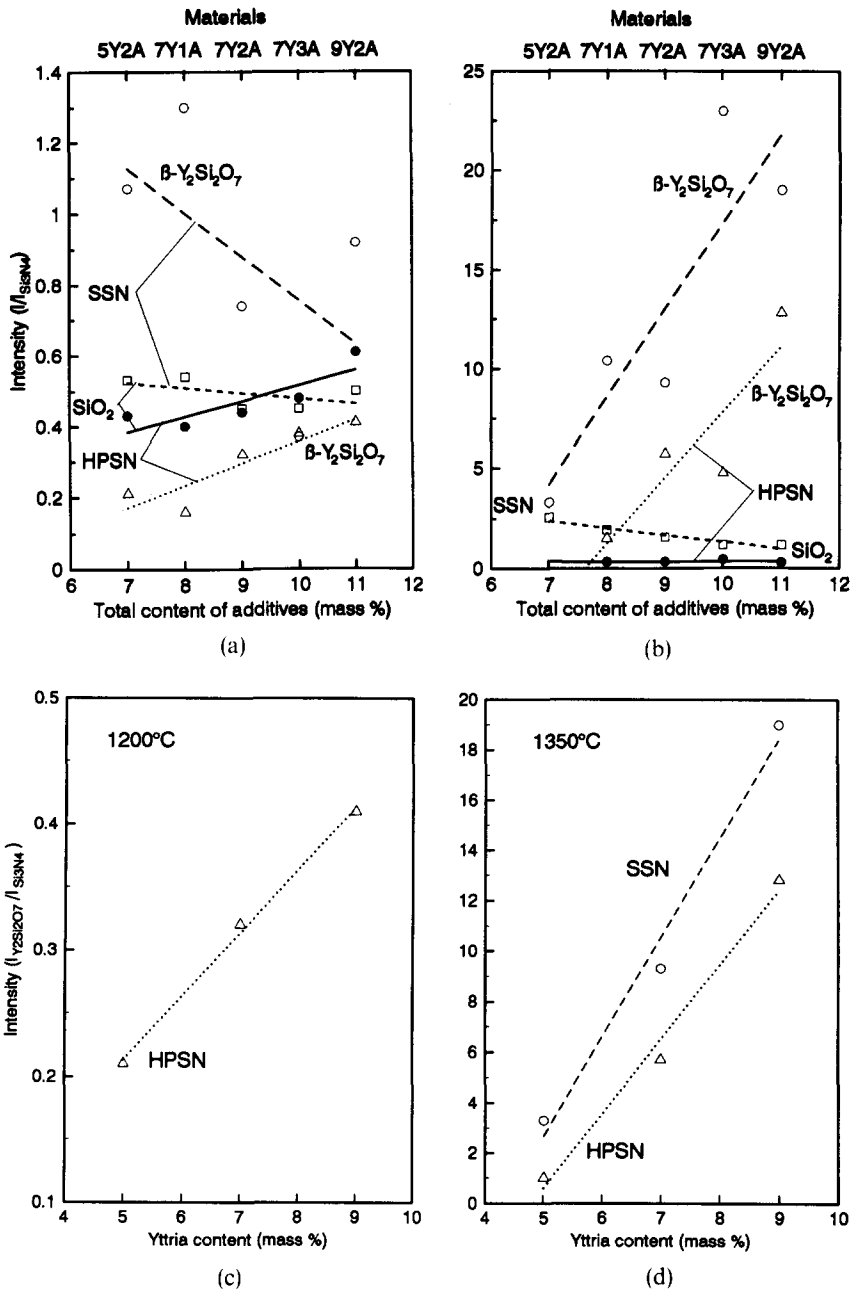

Fig. 5. Semiquantitative X-ray analysis of the surface layer of HPSN and SSN oxidized for 100 h at (a) 1200°C and (b) 1350°C as a function of the total additives content ((a) and (b)) and Y_2O_3 content ((c) and (d)).

yttrium disilicate and aluminosilicate glass, which were found in the oxide layer (Fig. 10).

The investigation of oxidation of yttrium oxynitrides[21] has demonstrated that the transformation of oxynitride phases to yttrium silicates is accompanied by a sharp increase of specific volume, which results in nonuniform internal stresses. The calculation reported in Ref. 20 shows that a total volume expansion of ~1% is close to the maximum level of strain that can be tolerated. A rough Hooke's law calculation for ceramics with $E = 300$ GPa provided in Ref. 20 shows that a total volume expansion of the sample of 1% would generate a stress of ~1000 MPa, which is of the same order of magnitude as the strength of the ceramics under study (Table 2). This can cause microcracking in the surface layers of the material which really occurs in SSN (Fig. 6(a)) at testing temperatures up to 1300°C. Above 1100°C cracking was observed only under short-term heating and was followed by healing of cracks during the isothermal heat treatment. But at the first stage of oxidation the oxide film does not cover the whole sample continuously (Fig. 6(c)) and allows the more intensive oxidation of some regions of the sample surface (Fig. 6(a)). Nonuniform discoloration of SSN specimens can be explained by large-scale inhomogeneities, caused by an irregular intergranular crystallization of the secondary phase.[22] At higher temperatures microcracking does not occur because of the softening of grain-boundary phases and stress relaxation. Only very thin microcracks resulting from the phase transformation in SiO_2 were found on the surface of samples. Temperature dependencies of strength and hardness of these

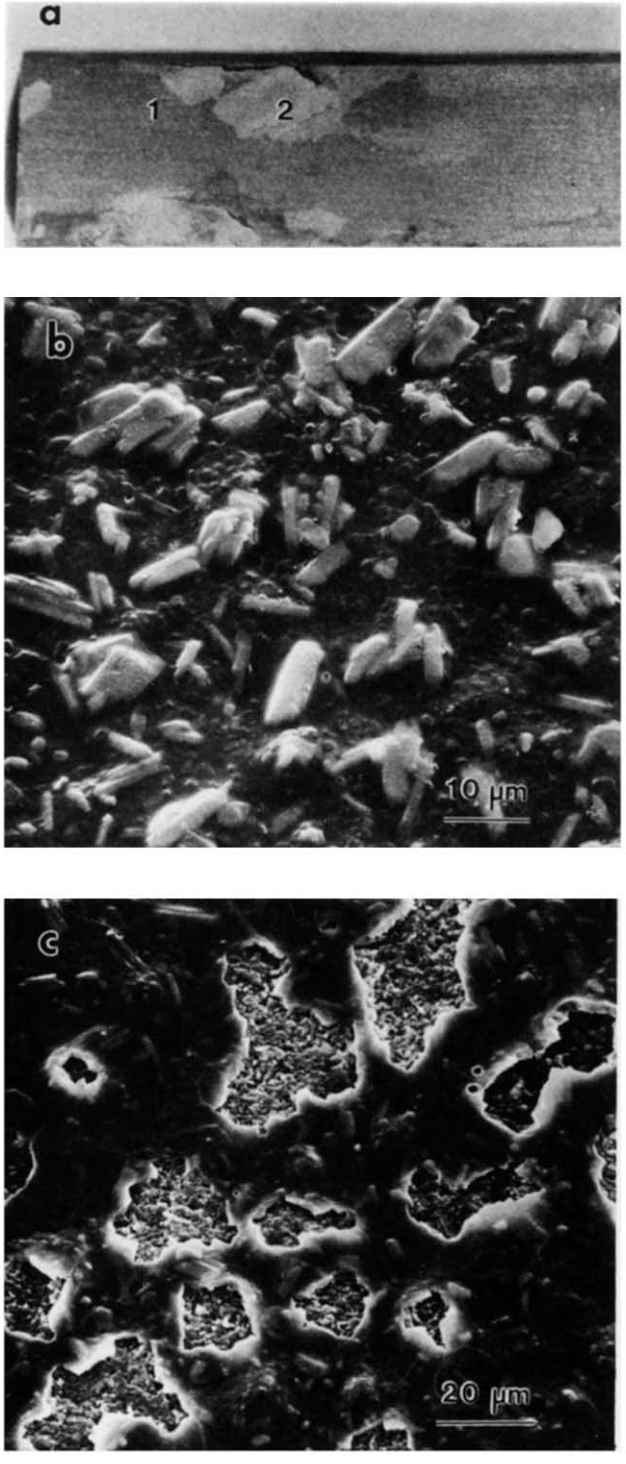

Fig. 6. (a) General view and (b) and (c) morphology of the surface of the SSN 9Y2A sample oxidized for 1 h at 1300°C: (b) region 1; (c) region 2.

ceramics[12] show that the softening of the intergranular phase, leading to the decrease of mechanical properties, occurs at ~1100°C. Therefore, above 1100°C the accommodation of the volume increase due to intergranular phase oxidation should be possible.

Oxidation tests under programmed heating rates did not reveal any significant mass gain of SSN at <1050°C. But all SSN samples showed discoloration, patch or spot formations, and some samples showed also surface cracking (Fig. 6(a)). Such low-

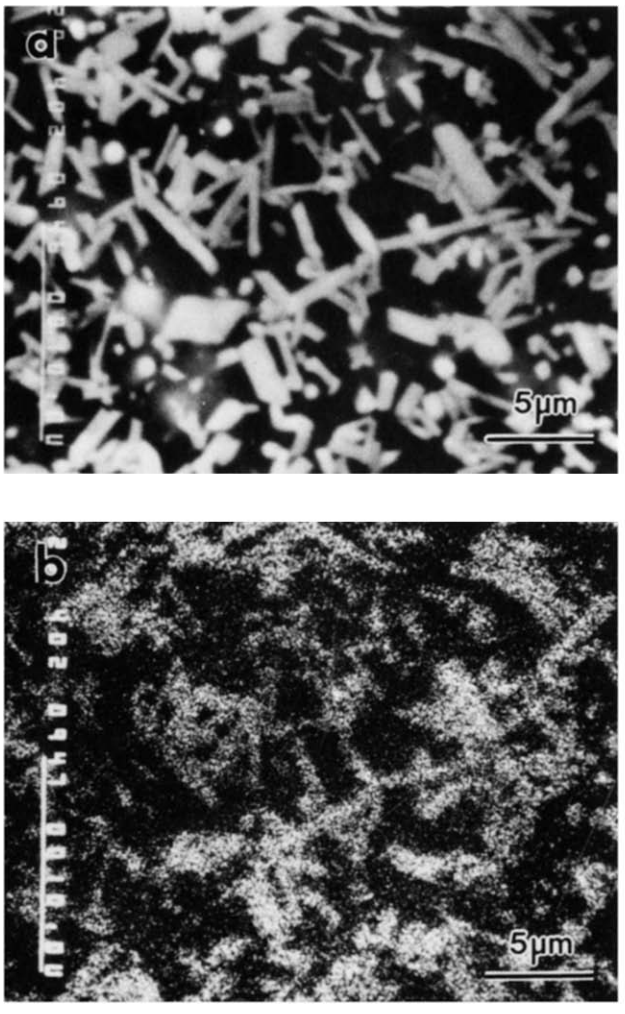

Fig. 7. Surface of an HPSN 5Y2A sample oxidized at 1300°C. (a) Secondary electron image; (b) X-ray map of Y. The white area corresponds to $Y_2Si_2O_7$ crystals.

temperature instability was observed for various Y_2O_3-doped silicon nitride ceramics.[2,10,20,23–26] The absence of detectable mass gain at these temperatures can be explained by a very low relative mass increase at oxidation according to the reactions (2)–(4) and by vaporization of WO_3 (see Section 4.2), compensating the mass gain due to the oxidation of grain-boundary phases.

In contrast, the HPSN samples having a higher SiO_2 content in the intergranular phase (Table 2) did not show any surface cracking, distortion or buckling and thus suggested the absence of oxidation instability at the intermediate temperatures. The higher SiO_2 content in HPSN has the following two consequences. The first is an increase of the viscosity and a decrease of diffusion rates in the intergranular phase, which lead to a decrease of the reaction rates. The second is an indirect one. The Al_2O_3 addition in the material incorporates during sintering into the Si_3N_4 according to the equation

$$z/2(Al_2O_3)_e + (6 - z/4)Si_3N_4 = Si_{6-z}Al_zN_{8-z}O_z + 3/4z(SiO_2)_e \quad (5)$$

Al_2O_3 and SiO_2 are also involved in the liquid phase.

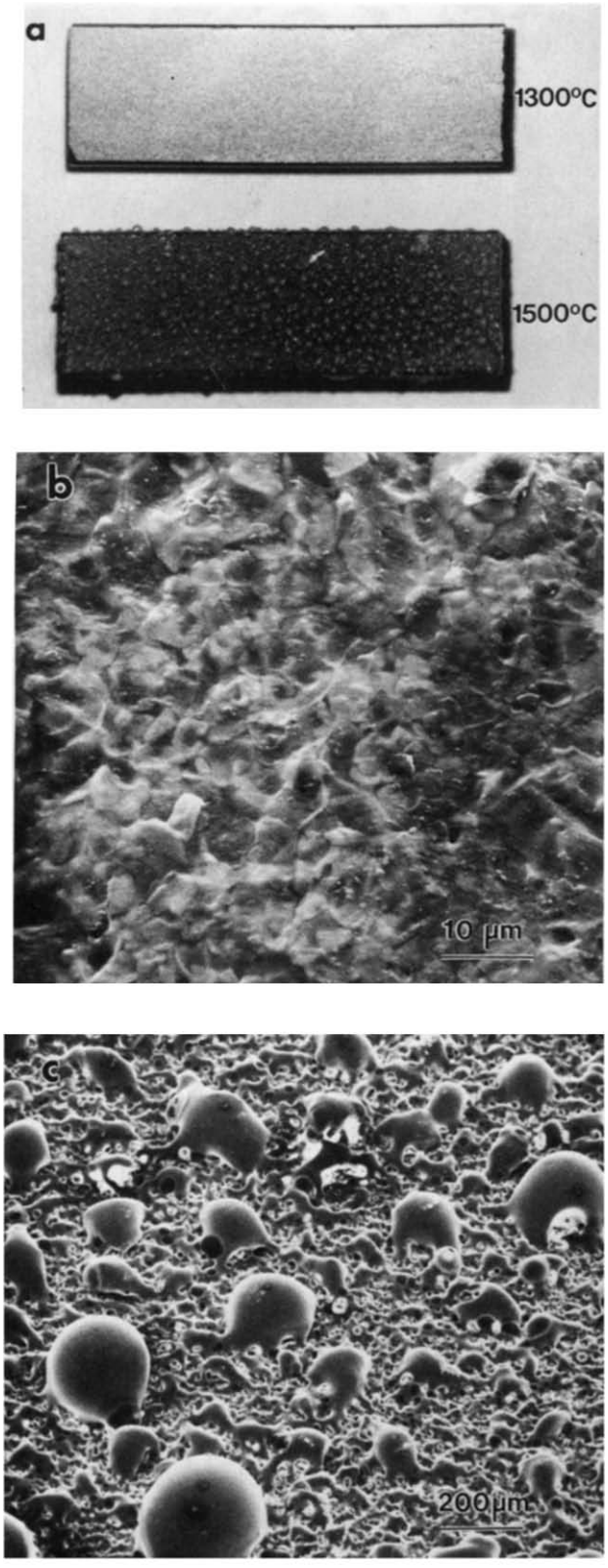

Fig. 8. (a) General view and (b) and (c) morphology of the surface of HPSN 7Y2A samples oxidized for (b) 75 h at 1300°C and (c) 8 h at 1500°C.

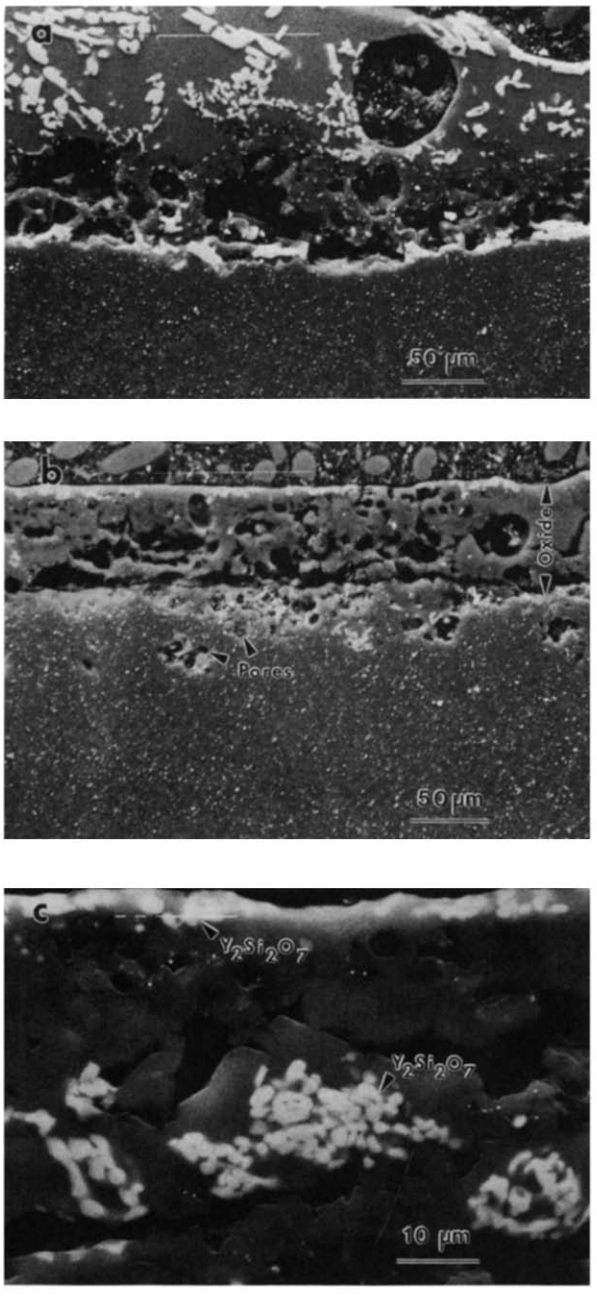

Fig. 9. Cross-sections of (a) HPSN 7Y1A and (b) and (c) 7Y3A samples oxidized for (a) 100 h and (b) and (c) 25 h at 1500°C.

TEM investigations of the intergranular glassy phase[27] show that a change of molar ratio of Al_2O_3 to a rare-earth oxide from 0·33 to 8·2 hardly changes the alumina content in the intergranular phase, because the main part of Al is incorporated in the β-Si_3N_4 grains. According to eqn (5) a higher alumina content in the initial composition leads to a higher SiO_2 content in the grain-boundary phase. This leads to decreasing oxidation below 1200°C (Figs 2 and 3) with increasing Al content. This change in the SiO_2 content can also explain changes in the $Y_2Si_2O_7/SiO_2$ ratio in the surface layer of the SSN materials oxidized at 1200°C (Fig. 5(a)). The ratio is about 2·6 for 7Y1A, 1·6 for 7Y2A and only 0·9 for 7Y3A ceramics.

The dependence of the oxidation mass gain (Figs 2 and 11) and the oxide layer phase composition (Fig. 5) on the additives content is strongly pronounced. As can be seen in Fig. 2, the lower additives content contributed to good oxidation resistance of HPSN in the temperature range II. A similar effect of additives was observed earlier for reaction-bonded,[26] sintered and hot-pressed[2] silicon nitride-

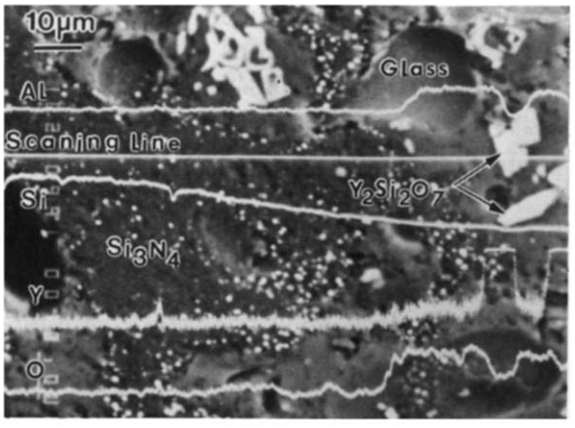

Fig. 10. Distribution of the main elements at the boundary oxide layer/substrate on the cross-section of an HPSN 7Y1A sample heated up to 1500°C.

based ceramics. Hot-pressed ceramics with a lower content of additives were more stable under oxidation above 1350–1400°C than additive-rich ceramics (Figs 2, 3(b) and 11), probably because of the protective effect of the cristobalite layer formed. These experiments, together with the data presented in Refs 25 and 26, offer clear evidence that an increase in the total additives content increases oxidation rates at high temperatures.

This result is in agreement with the assumption of Andrews & Riley[19] that the solution of cristobalite in a liquid silicate phase is an important factor in the overall rate-controlling process. The higher amount of additives contributed to lower cristobalite content in the oxide scale (Fig. 5(b)) due to diffusion of Y and Al cations to the surface and formation of glassy and crystalline silicate phases. It has been shown[2] that Al_2O_3 dissolved in the silicate phase hinders crystallization, thereby promoting glass formation. The higher content of yttria in ceramics increases the quantity of β-$Y_2Si_2O_7$ in the oxide layer at high temperatures (Fig. 5(d)). It is known[15] that the diffusion rate of oxygen in silicates is much higher than in pure SiO_2. An increase in the oxygen transport rate will increase the overall oxidation rate. Thus, the more strongly fluxed the surface silicate layer by dissolved constituents from the substrate (Y, Al), the lower the viscosity of the glass and the material's resistance to oxidation.

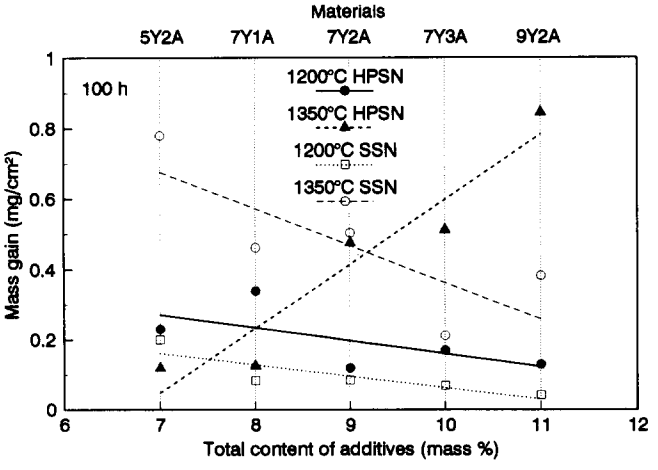

Fig. 11. Mass gain of HPSN and SSN samples oxidized 100 h at 1200 and 1350°C versus additives content.

In the temperature range II (Fig. 2) the dependence of the oxidation resistance of different ceramics (Fig. 11) and the amount of crystalline phases on the additives content is much more complex. The higher content of alumina in SSN decreases the temperature of the liquid-phase formation and increases the oxidation resistance of an intergranular phase at the intermediate temperatures,[2] resulting in the lower content of yttrium silicate in the oxide scale at 1200°C (Fig. 5) and lower oxidation rates up to 1350°C (Fig. 11). For HPSN ceramics the influence of additives at 1200°C was to decrease the mass gain (Fig. 11) but to increase the content of crystalline oxide phases content on the surface of ceramics (Fig. 5(a)).

Thus, the oxidation resistance at low and intermediate temperatures (ranges I and II) is determined by the phase composition and presence of unstable oxynitride phases. On the other hand, the total content of additives in ceramics (and consequently in the oxide layer) determines the oxidation behaviour at high temperatures (range III).

Above 1300°C, when the oxidation of Si_3N_4 grains is more intense, the alumina content in the surface increases with increasing Al content in the material and the oxidation rate grows (Figs 2 and 3).

The formation of a protective SiO_2 scale on the surface of HPSN samples after a few minutes of oxidation leads to a high resistance for HPSN, for which inward diffusion of oxygen is rate limiting. An acceleration of diffusion of dopants and impurity cations to the reaction interface with the temperature increase leads to the formation of a protective dense and coherent oxide layer also on the surface of SSN ceramics. However, the formation of a thicker oxide layer, in comparison with HPSN, containing also a lot of cracks and bubbles was observed. Figure 5 illustrates the difference in α-cristobalite and β-$Y_2Si_2O_7$ amounts on the surface of hot-pressed and sintered samples.

The oxidation behaviour above 1400°C was similar for both groups of materials. After a short time interval the concentration of impurities in the oxide scale reached a sufficient level to dissolve the protective cristobalite layer formed at lower temperatures. The low viscosity silicate film (Fig. 8(a) and (c)) then evidently became less protective and the materials oxidized almost linearly.

4.2 Effect of tungsten compounds

As already indicated, the largest part of W present in these Si_3N_4 ceramics is in a reduced state. This fact is

in agreement with thermodynamic calculations.[21] As the oxygen potential increases in the surface layer, W should be present as the oxide dissolved in the liquid silicate phase. But the WDS showed a very low W content in oxide films, perhaps owing to vaporization of volatile tungsten oxides. However, W was present beneath the oxide layer in the Si_3N_4 matrix (white points in the lower part of Fig. 12(b) and (c)), showing no preferable oxidation. Tungsten compounds' oxidation in accordance with reactions

$$WC + 2O_2 = WO_3 + CO \quad (6)$$

and

$$WSi_2 + 7O_2 = 2WO_3 + 4SiO_2 \quad (7)$$

starts at lower temperatures than the oxidation of silicon nitride, and in the low temperature range I the mass loss due to WC and WSi_2 oxidation can exceed the mass gain due to Si_3N_4 oxidation. Such an effect was observed for 5Y2A HPSN specimens at temperatures up to 1130°C[28] and for Al_2O_3-doped SiC containing 4% WC even at temperatures up to 1400°C.[26] Simple calculations using eqn (6) show that the WC oxidation and vaporization of oxidation products from the oxidized layer of ~15 μm at a WC content of 2 mass% result in a mass loss of ~0·1 mg/cm^2. This value is comparable with mass gains due to oxidation (Fig. 11). At very high temperatures a thick silicate layer retards the W transport to the oxide/gas interface and the mass gain due to Si_3N_4 oxidation exceeds substantially the mass loss due to WO_3 evaporation.

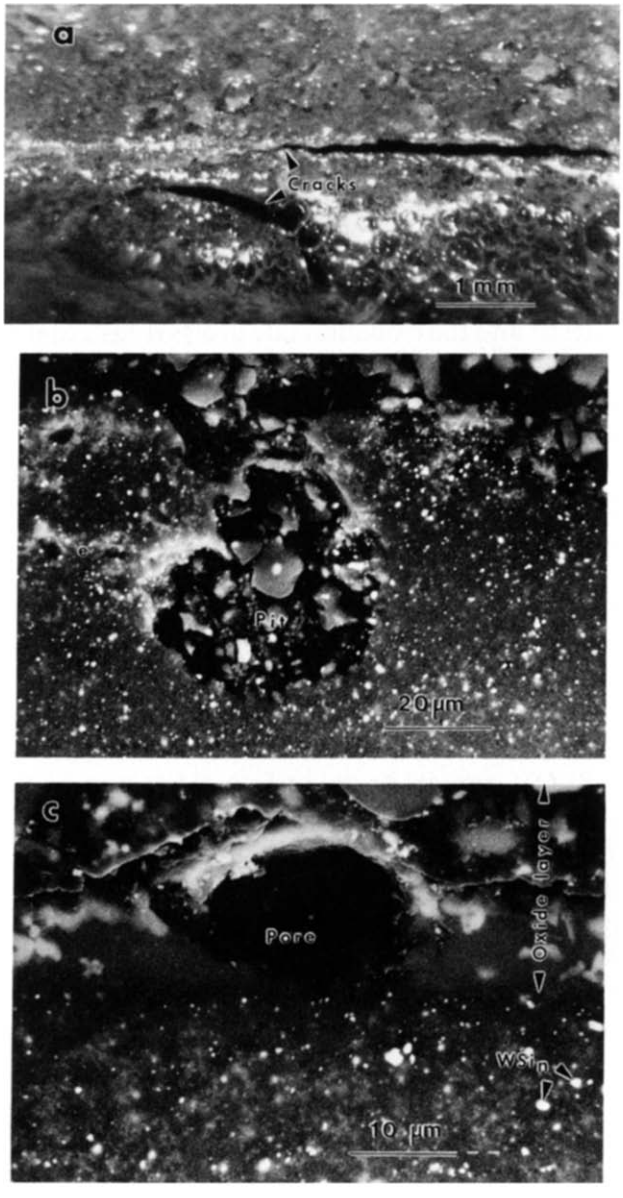

Fig. 12. (a) Surface and (b) and (c) cross-sections of the HPSN 7Y3A samples oxidized for (a) and (b) 25 h at 1500°C and (c) 100 h at 1300°C.

Thus, it should be taken into consideration that the results of mass change measurements reflect the contributions from at least two simultaneous processes, one leading to the mass gain (Si_3N_4 or Si–Y oxynitrides oxidation) and the other resulting in the mass loss (e.g. WO_3 vaporization) of the samples.

The lower mass gain (Fig. 11) and the more severe oxidative degradation of the surface of SSN in comparison with HPSN can then be explained in terms of the more intensive WO_3 vaporization. The presence of WC instead of WSi_2 in SSN leads, as can be calculated from eqns (6) and (7), to a ~40% higher mass loss during oxidation. The formation of a non-protective oxide layer (Fig. 6(c)) at the first stage of oxidation facilitates the evolution of gaseous tungsten oxides and leads to more severe mass loss of ceramics.

4.3 Oxide scale structure and surface degradation

Oxide scales, in general, were formed at >1200°C with important microstructural variations from their surface to the reaction interface, irrespective of composition and nature of the material. The β-$Y_2Si_2O_7$ crystals are present on the oxide surface and in the oxide/substrate interface (white in Figs 9(c) and 10), but usually do not appear in the mid-zone of the oxide film, which is only constituted of α-cristobalite and glassy phase. A pure cristobalite layer on the boundary between the silicate oxide film and Si_3N_4 substrate was found only at 1200–1300°C. At higher temperatures dissolution of pure SiO_2 in a silicate phase probably occurred, and a glassy phase with relatively uniformly distributed aluminium was found (Fig. 10). The formation of a porous layer between Y-rich layers and/or on the oxide/bulk material interface was observed after the oxidation above 1300°C (Fig. 9), so that the film ceases only locally to be anchored to the ceramics. In some cases cracks can propagate through this porous layer after cooling, resulting in the spalling of the oxide film (Fig. 12(a)). The formation of a porous layer between the oxide scale and bulk material could be a reason for the non-parabolic oxidation kinetics of ceramics at higher temperatures. The formation of cavities on the boundary oxide layer/bulk material diminishes the area over which Y atoms

can move into the scale as ions, and oxygen can move to the reaction interface, and thus the effective area available for the oxidation process is reduced.[29] This causes the oxidation rate to fall off after 20–70 h more rapidly (the curves in Fig. 3(a)) than the parabolic law would predict. Such retardation of the oxidation process was also observed in Refs 4, 16 and 23, and explained in terms of the formation of bubbles in the oxide scale.

As can be seen in Fig. 12, oxidation of all materials studied above 1400°C leads to the appearance of pores in the subsurface layer (Fig. 9(b)), as well as formation of pits (Fig. 12(b)) and large pores (Fig. 12(c)) on the boundary oxide layer/bulk material. The cracking and spalling of the oxide scale after oxidation at 1500°C and cooling to room temperature was also observed (Fig. 12(a)).

4.4 Temperature regimes of oxidation mechanisms

On the basis of the results obtained and reported in this study, it should be discussed how the oxidation of Si_3N_4-based ceramics is controlled by different mechanisms depending on the temperature. The foregoing discussion of the oxidation behaviour defined three temperature ranges: below ~1050°C (I), 1100–1300°C (II) and above ~1350°C (III). The precise boundaries of these temperature ranges depend on the additives content and phase composition of Si_3N_4 ceramics.

As has been shown, only oxidation of tungsten compounds and Si–Y oxynitrides occurred at the lowest temperatures (temperature range I). The rate-controlling step is probably the inward diffusion of oxygen through grain boundaries[30] and, later, through cracks. The boundary of the first temperature range is the beginning of the pronounced oxidation of Si_3N_4.

In the temperature range II a gradual change in oxidation behaviour takes place. The literature[10,14,19,30] gives a fairly good explanation of the mechanisms involved. The parabolic oxidation at these temperatures is explained by the formation of silica. With time the thickness of the silica layer increases and progressively the specimen is covered with a protective scale. So the grain boundaries are closed by a SiO_2-rich layer which stops the internal oxidation.

The comparison of the parabolic rate constants k_p derived from eqn (1) for 7Y3A HPSN with the values obtained by Bellosi *et al.*[10] for materials of a similar composition (Fig. 4(b)) shows a good correlation. However, somewhat lower k_p and apparent activation energy values (compared with the data in Table 1) were measured in the present experiments.

The present experiments corroborated the observations of Andrews & Riley[19] that beyond a critical temperature (the boundary between the ranges II and III), which probably corresponds to the eutectic temperature of the silicate layer formed, an increase of oxidation rates occurred. The reason for the change in oxidation behaviour must be related to the changed composition and morphology of the oxidation products (Fig. 8) above the eutectic temperature. The liquid formation permits the dissolution of SiO_2 and replacement of a protective continuous cristobalite film by localized crystal growth. Enhanced rates of oxidation are characterized by the transition from parabolic to near linear oxidation kinetics.

5 Conclusions

(1) The oxidation resistance of $Y_2O_3 + Al_2O_3$-containing silicon nitride is strongly dependent on the content of additives and processing conditions, resulting in different phase compositions of materials.

(2) Gas-pressure sintered ceramics containing crystalline yttrium–silicon oxynitrides in the intergranular phases showed instability at the intermediate temperatures and lower oxidation resistance than hot-pressed ceramics prepared from the same powder mixtures. Hot-pressed ceramics exhibited excellent resistance to oxidation by air at temperatures up to 1400–1450°C, because of the formation of a protective oxide layer.

(3) Samples with the higher amount of additives were more stable under the oxidation up to 1350°C; the reverse was the case at higher temperatures. Thus, it appears likely that additive-rich ceramics will be employed predominantly in applications involving use temperatures below ~1300°C. On the other hand, ceramics with the lowest additives content have better oxidation resistance at the highest temperatures.

(4) The addition of Al_2O_3- to Y_2O_3-doped ceramics is not sufficient to overcome the low-temperature instability of these materials. The formation of stable intergranular phases during sintering is the fundamental condition for their good oxidation resistance.

(5) Changes of oxidation kinetics and mechanisms in different temperature ranges were observed under the experimental conditions:

—Below ~1050°C only oxidation of Si–Y oxynitrides and W compounds takes place. The rate-controlling step is the inward diffusion of oxygen through grain boundaries.

—In the range 1100–1350°C oxygen diffusion through a protective SiO_2 or silicate layer is the rate-limiting step for parabolic oxidation.

—Above ~1350°C the formation of a liquid silicate phase and dissolution of the protec-

tive SiO_2 film in this liquid are responsible for the markedly faster oxidation rate.

(6) The degradation of the surface layer and formation of large flaws was observed for HPSN and SSN at >1400°C. Cracking of the surface along the boundaries of oxidized discoloured regions was found for SSN at the intermediate temperatures. At higher temperatures the SSN oxidation mechanism is the same as for HPSN, but usually enhanced oxidation rates are observed.

(7) Oxide scales exhibit a layered structure with microstructural variations from their surface to the reaction interface. This has been found for all compositions studied, almost independently of oxidation temperature.

(8) The content of α-cristobalite and β-$Y_2Si_2O_7$ in the oxide scale is dependent on ceramics composition.

Acknowledgements

The authors are grateful to Dr A. D. Vasil'ev and Mr V. V. Kovylyaev from the Institute for Problems of Materials Science (Kiev, Ukraine) for help with electron microprobe analysis. Dr Yury Gogotsi gratefully acknowledges the receipt of a Research Fellowship from the Alexander von Humboldt Foundation, under which this work was undertaken at the University of Karlsruhe.

References

1. Hasegawa, Y., Tanaka, H., Tsutsumi, M. & Suzuki, H., Oxidation behaviour of hot-pressed Si_3N_4 with addition of Y_2O_3 and Al_2O_3. *Yogyo-Kyokai-Shi*, **88** (1980) 292–7.
2. Quackenbush, C. L. & Smith, J. T., Phase effects in Si_3N_4-containing Y_2O_3 or CeO_2: II, Oxidation. *Am. Ceram. Soc. Bull.*, **59** (1980) 533–7.
3. Govila, R. K., Strength characterization of yttria/alumina-doped sintered silicon nitride. *Int. J. High Tech. Ceram.*, **3** (1987) 179–97.
4. Nickel, K. G., Danzer, R., Schneider, G. & Petzow, G., Korrosion und Oxidation von Hochleistungskeramik. In *Symp. Materialforschung*, Hamm/Westfallen, 12–19 September 1988, pp. 611–30.
5. Wang, L., He, C. & Wu, J. C., Oxidation of sintered silicon nitride materials. In *Proc. 3rd Int. Symp. Ceramic Materials and Components for Engines*, ed. V. J. Tennery. American Ceramic Society, Westerville, OH, 1989, pp. 604–11.
6. Wakamatsu, M., Takeuchi, N., Hattori, T., Watanabe, K. & Makoto, I., Oxidation of sintered Si_3N_4 at 1400°C in oxygen atmosphere. In *Proc. UNITECR '89*. American Ceramic Society, Westerville, OH, 1989, pp. 1694–703.
7. Wakamatsu, M., Takeuchi, N., Shimuzu, S., Hattori, T., Oyama, M., Nanri, H. & Ishida, S., Oxidation of sintered Si_3N_4 during heating up to 1600°C under oxygen atmosphere. In *Proc. MRS Int. Symp. Composites/Corrosion/Coating of Advanced Materials*, Vol. 4, ed. M. Doyama *et al.* MRS, 1989, pp. 283–8.
8. Echeberria, J. & Castro, F., Microstructure of the oxide layers produced during oxidation of silicon nitride. In *Euro-Ceramics*, Vol. 3, ed. G. de With, R. A. Terpstra & R. Metselaar. Elsevier, London, 1989, pp. 3.527–32.
9. Echeberria, J. & Castro, F., Comparison between continuous and cyclic oxidation of fully dense Si_3N_4 + 1 w/o Y_2O_3. In *Proc. 11th Risø Int. Symp. on Metallurgy and Materials Science*, ed. J. J. Bentzen *et al.* Roskilde, 1990, pp. 249–55.
10. Bellosi, A., Babini, G. N., Li-Ping, H. & Xi-Ren, F., Phase effects on oxidation resistance in Si_3N_4–Al_2O_3–Y_2O_3. *Mat. Chem. Phys.*, **26** (1990) 21–33.
11. Kim, H.-E. & Moorhead, A. J., Strength of hot isostatically pressed Si_3N_4 after heat treatment in Ar–O_2 and H_2–H_2O. *J. Am. Ceram. Soc.*, **73** (1990) 1443–5.
12. Gogotsi, Yu. G., Grigorjew, O. N. & Jaroschenko, V. P., Mechanische Eigenschaften von heißgepreßtem Siliziumnitrid bei hohen Temperaturen. *Silikattechnik*, **41** (1990) 156–60.
13. Luthra, K. L., Some new perspectives on oxidation of silicon carbide and silicon nitride. *J. Am. Ceram. Soc.*, **74** (1991) 1095–103.
14. Andrews, P. & Riley, F. L., Silicon nitride oxidation/reoxidation. *J. Eur. Ceram. Soc.*, 7 (1991) 125–32.
15. Kingery, W. D., Bowen, H. K. & Uhlmann, D. R., *Introduction to Ceramics*. Wiley, New York, 1976.
16. Ernstberger, U., Grathwohl, G. & Thümmler, F., High-temperature durability and limits of sintered and hot-pressed silicon nitride materials. *Int. J. High Tech. Ceram.*, **3** (1987) 43–61.
17. Herrmann, M., Grigor'ev, O. N., Gogotsi, Yu. G. & Yaroshenko, V. P., Sintered ceramics based on silicon nitride. In *Abstr. All-Union Conf. on Constructions and Manufacturing of Parts from Inorganic Materials*. Moscow, 1990, pp. 6–7 (in Russian).
18. O'Meara, C., Sjöberg, J. & Dunlop, G., Oxidation of pressureless sintered Si_2N_2O materials. *J. Eur. Ceram. Soc.*, 7 (1989) 369–78.
19. Andrews, P. & Riley, F. L., The microstructure and composition of oxide films formed during high-temperature oxidation of a sintered silicon nitride. *J. Eur. Ceram. Soc.*, **5** (1989) 245–56.
20. Patel, J. K. & Thompson, D. P., Further studies of the low-temperature oxidation problem in yttria-densified silicon nitride ceramics. In *Proc. 3rd Int. Symp. Ceramic Materials and Components for Engines*, ed. V. J. Tennery. American Ceramic Society, Westerville, OH, 1989, pp. 987–96.
21. Williams, R. O. & Tennery, V. J., Phase equilibria in the oxidation of impure silicon nitride. *J. Mater. Sci.*, **14** (1979) 1567–71.
22. Leng-Ward, G. & Lewis, M. H., Irregular intergranular crystallization of $Y_2Si_2O_7$. *J. Am. Ceram. Soc.*, **75** (1992) 257.
23. Steinmann, D., Untersuchung des langsamen Rißwachstums von heißgepreßtem Siliziumnitrid (HPSN) bei hohen Temperaturen. *Sprechsaal*, **121** (1988) 909–20.
24. Govila, R. K., Fracture and intermediate temperature instability in yttria-doped hot-pressed silicon nitride. *Am. Ceram. Soc. Bull.*, **65** (1986) 1287–92.
25. Hirosaki, N., Akimune, Y., Ogasawara, T. & Odaka, A., Effect of additive amount of oxidation of Y_2O_3–Nd_2O_3-doped silicon nitride. *J. Mater. Sci. Lett.*, **10** (1991) 753–5.
26. Gogotsi, Yu. G. & Lavrenko, V. A., *Corrosion and its Effect on Properties of Engineering Ceramics*. Springer, Heidelberg, 1992.
27. Taut, Ch. & Herrmann, M., Oxidation of rare-earth oxides containing Si_3N_4. *J. Mater. Sci. Lett.*
28. Gogotsi, Yu. G. & Porz, F., Oxidation of particulate-reinforced Si_3N_4–TiN composites. *Corrosion Sci.*, **33** (1992) 627–40.
29. Evans, U. R., *The Corrosion and Oxidation of Metals*. Arnold, London, 1960.
30. Desmaison-Brut, M. & Billy, M., High temperature corrosion of hot pressed silicon nitride. In *High Temperature Corrosion of Technical Ceramics*, ed. R. J. Fordham. Elsevier, London, 1990, pp. 131–40.